

ASSESSMENT OF SINGLE CELL VIABILITY FOLLOWING LIGHT-INDUCED ELECTROPORATION THROUGH USE OF ON-CHIP MICROFLUIDICS

Justin K. Valley¹, Hsan-Yin Hsu, Steven Neale, Aaron T. Ohta, Arash Jamshidi, and Ming C. Wu¹
¹Berkeley Sensor & Actuator Center, Department of Electrical Engineering and Computer Sciences
 University of California, Berkeley, USA

ABSTRACT

The high throughput electroporation of single cells is important in applications ranging from genetic transfection to pharmaceutical development. Light-induced electroporation using optoelectronic tweezers (OET) shows promise towards achieving this goal. However, cell viability following light-induced electroporation has yet to be shown. Here we present a novel OET device which incorporates microfluidic channels in order to assess the viability of single cells following light-induced electroporation. Monitoring of single cell electroporation and viability is achieved through the use of fluorescent dyes which are exchanged using the integrated fluidic channels. The successful reversible electroporation of HeLa cells is shown.

INTRODUCTION

Electroporation is a widely used technique for the introduction of exogenous molecules across the cell membrane through the use of external electric fields. If the field the cell is subjected to is large enough, the cell's membrane will porate, allowing molecular exchange with the external environment. The field can be properly tuned so that these pores can then reseal. This technique is largely used for genetic transfection and fluorescent tagging.

Conventional electroporation techniques are, however, limited by either low throughput or limited selectivity. Due to this, there has been increasing interest in creating a system capable of performing high throughput electroporation with single cell selectivity for on-chip transfection and cell-monitoring studies [1-3]. We have recently reported on the use of OET to achieve light-induced electroporation [4]. As shown in Figure 1, in this scheme, we use light-induced dielectrophoresis to manipulate individual cells in parallel and, then, by increasing the bias, we selectively electroporate the illuminated cells. By combing OET with electroporation, a high throughput, high selectivity assay can be performed.

Optoelectronic tweezers uses patterned light to alter the conductivity of a photosensitive film to create localized electric field gradients. These gradients result in a dielectrophoretic (DEP) force on particles in the vicinity. Figure 2 shows the electric field distribution created by illuminating a region of the photosensitive film. Note the concentration of electric field and creation of localized electric field gradients at the center of the x-axis where the 20 μm light spot is incident. Because of the low light power necessary for actuation, compared to the more traditional optical tweezers, thousands of simultaneous traps can be created and manipulated in parallel [5].

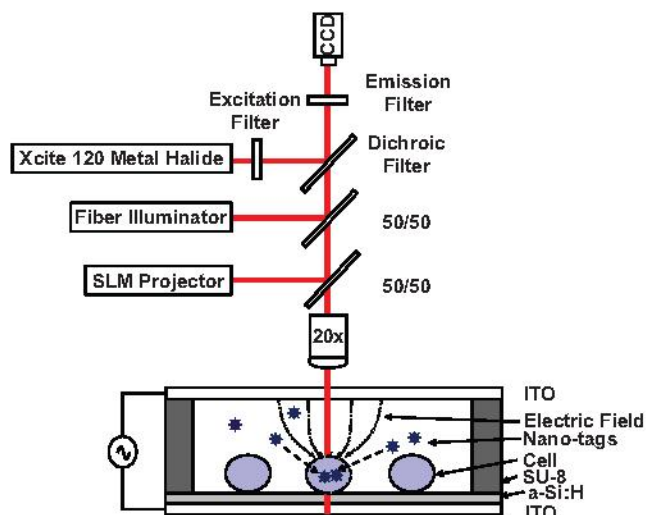


Figure 1: Experimental setup and schematic showing electroporation mechanism. Electric field is concentrated across the illuminated cell resulting in electroporation. A series of filters are used to select the appropriate fluorescent dye to monitor. Fluid exchange occurs through the use of a syringe pump (not pictured).

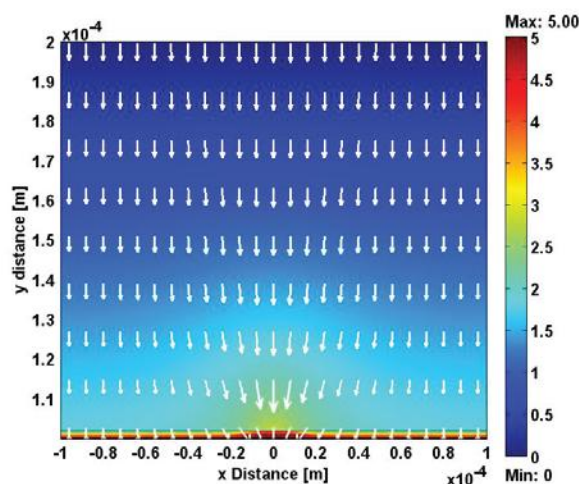


Figure 2: Electric field profile created by illumination in the OET device at center of x-axis. Arrows correspond to electric field, while the surface plot corresponds to electric potential for a 5 V amplitude signal. Note how localized electric field gradients and electric field concentration occurs in the illuminated region.

When a cell is illuminated by the projected light in the OET device, the electric field is concentrated across it. If the electric field is large enough, the cell's membrane will form nanoscopic pores allowing exogenous molecules to enter the cell (Figure 1). In this manner, one

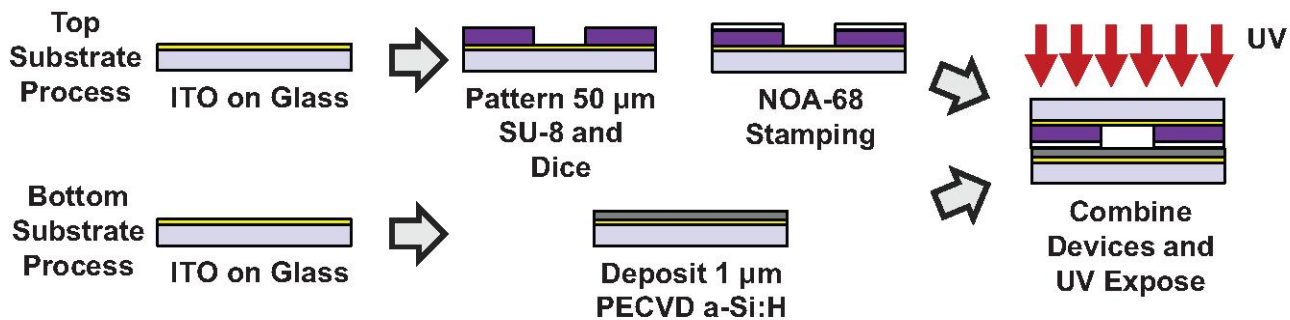


Figure 4: Fabrication of OET with integrated microfluidic channels. Channels are defined in SU-8 on the topside OET substrate and bonded to the bottom OET substrate using a UV-curable epoxy.

can individually select and electroporate cells in parallel.

However, until now, the reversible electroporation of cells has not been demonstrated in this device. Reversible electroporation refers to the ability of the pores in an electroporated cell to reseal. This process typically takes on the order of minutes to tens of minutes [6] and is highly dependent on the electric field dose applied during the electroporation process. A common method for the investigation of reversible electroporation is the use of fluorescent dyes [7]. First a cell is electroporated in the presence of a dye which causes successfully electroporated cells to fluoresce. Next, the solution surrounding the cells is replaced with a solution containing another dye which indicates whether the electroporated cell is viable. For cells not adhered to the surface, this procedure requires the use of on-chip microfluidic channels. Here we present a process by which the OET device is integrated with lithographically defined channels and demonstrate its capability by showing that reversible electroporation can be obtained.

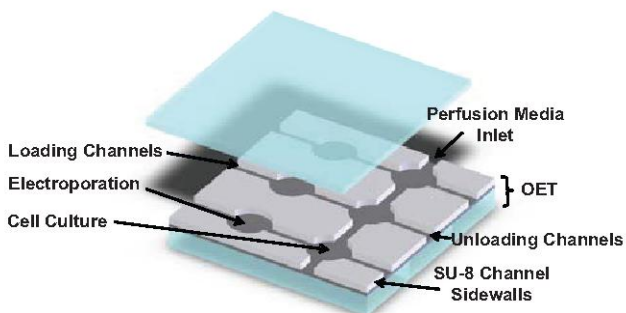


Figure 3: Concept overview of OET-based electroporation assay. Cells are electroporated in parallel with single cell selectivity in lithographically defined compartments and then moved into perfusion chambers allowing for subsequent cell culture.

FABRICATION

The integration of microfluidic circuits with the OET device will allow for applications ranging from on-chip sorting to on-chip cell culture (Figure 3). We have developed a process that allows lithographically defined channels to be integrated with the OET electroporation device. This process needs to allow for arbitrary top and bottom substrates. This is because the OET device requires a transparent conductive top surface and a

photosensitive bottom substrate. Additionally, in order to accommodate cells, the channel height must be relatively thick ($\sim 50 \mu\text{m}$) and the channel material must be non-conductive. SU-8 lends itself well to this task due to its ability to easily form high-aspect ratio, permanent, structures. The process is depicted in Figure 4.

Indium tin oxide (ITO) (300 nm) coated glass serves as the top and bottom OET surface. The bottom substrate is coated with a $1 \mu\text{m}$ layer of PECVD a-Si:H (100 sccm 10%SiH₄:Ar, 400 sccm Ar, 900 mTorr, 350°C, 200 W). The top substrate is patterned with $50 \mu\text{m}$ of SU-8 (Microchem, SU-8 2050) which defines the channel geometry. Both substrates are then diced into 2x2 cm chips using a dicing saw (Esec 8003). Fluidic input and output ports are then drilled into the topside device with a drill press and 0.75 mm drillbit.

A $20 \mu\text{m}$ layer of UV-curable epoxy (Norland, OA-68) is then spin coated (4000 RPM, 2 min.) on a dummy wafer. A block of polydimethylsiloxane is used to stamp the NOA-68 from the dummy wafer to the SU-8 channels. This results in a $\sim 15 \mu\text{m}$ layer of NOA-68 on the top of the SU-8 channel sidewalls. Finally, the top and bottom OET substrates are combined and the epoxy is cured using a handheld UV gun (Norland, Opticure-4, 10sec). No alignment is needed in this case as the bottom substrate is featureless. The combination of the two substrates can be accomplished by hand or through the use of a flip-chip bonder. Fluidic access connections are then attached to the ports on the topside of the device with additional NOA-68.

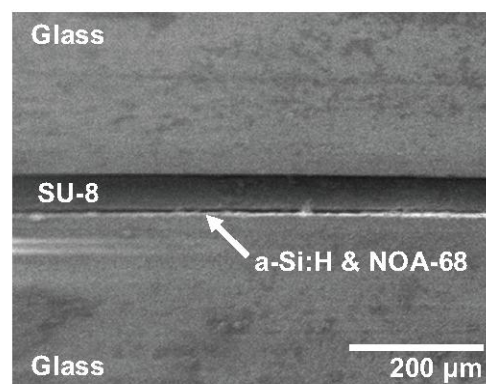


Figure 5: SEM of cross section of OET device with integrated SU-8 microfluidic channels.

Figure 5 shows an SEM cross-section of the described device showing the top and bottom substrates, SU-8, a-Si:H, and NOA-68. Figure 6 is a picture of the completed device.

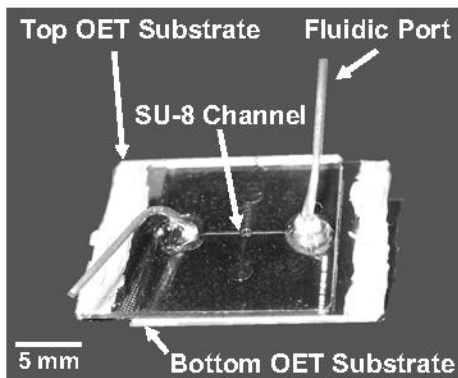


Figure 6: Picture of completed device. The top and bottom OET substrates are bonded together using a UV curable epoxy resulting in sealed microfluidic channels. Fluids are introduced through fluidic ports.

EXPERIMENTAL

For many applications (e.g. transfection), the cell must remain viable following electroporation (i.e. reversible electroporation). For a demonstration of the integrated device, we assess the viability of a single cell following light-induced electroporation. In order to show this, we use the technique mentioned before using two cellular dyes. The first dye, Propidium Iodide (PI) (Invitrogen), is a membrane impermeant dye. However, if the dye enters the cell, it binds to DNA and fluoresces red. It is an indicator of successful electroporation. The second dye, Calcein AM (CaAM) (Invitrogen), passively diffuses across the cell membrane. Once in the cytosol, it interacts with enzymes in the cell and produces a green fluorescent molecule which is membrane impermeant. Strong green fluorescence in the presence of CaAM means that the cell's membrane is intact and that the intracellular contents contain the necessary enzymes to catabolize the CaAM. If these two conditions are met, it is a strong indicator of cellular viability.

Since CaAM is membrane permeant it is necessary to introduce it following electroporation, necessitating the use of microfluidic channels. To demonstrate successful reversible electroporation, we first select a cell, electroporate it in the presence of PI, and then exchange the media with a solution containing CaAM. If the cell fluoresces both red and green at the completion of the experiment, the cell has been reversibly electroporated.

HeLa cells were washed three times in and suspended in electroporation buffer (Cytopulse® Electroporation Medium, 10 mS/m) at a cellular concentration of 2×10^6 /mL. Due to the presence of large electrical fields during electroporation (kV/cm), joule

heating in the liquid is an issue. Small temperature changes can reduce cellular viability significantly. Since joule heating is directly proportional to liquid conductivity, it is advantageous to use lowly conducting media.

PI dye was added to the cellular solution to achieve a concentration of 2 μ M. CaAM dye at 6 μ M was also prepared to be introduced later. The cell and PI solution was then introduced into the device via a syringe pump. The CaAM solution was also connected to the device to be introduced later.

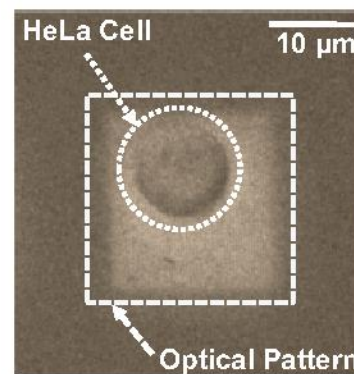


Figure 7: Bright-field image of HeLa cell under test in OET device with applied optical pattern. Cells are suspended in Cytopulse® Electroporation media (8 mS/m).

An individual HeLa cell is selected and a light pattern is generated to illuminate it (Figure 7). After initial positioning at low voltage (4 Vppk), the cell does not exhibit any fluorescence (Figure 8). This is because the fields the cell experiences during movement are less than that required to porate the cell membrane. However, once the electroporation bias is applied (20 Vppk), the critical field required to porate the membrane is surpassed and the cell uptakes PI and fluoresces accordingly. No CaAM fluorescence is seen at this stage as this dye is not currently present in the solution (Figure 8). Next the media surrounding the cells is exchanged, via the fluidic channels using a syringe pump, with the CaAM solution. After fluid exchange, the cells are incubated for 15 minutes to allow the CaAM to diffuse into the cells. After incubation, the cell now exhibits both PI and CaAM uptake (Figure 8). This means that the cell's membrane has resealed following electroporation and that it contains the appropriate enzymes necessary to catabolize the CaAM into its fluorescent derivative. Therefore, successful reversible electroporation has occurred.

CONCLUSION

We have demonstrated the integration of microfluidic chambers onto the OET device to demonstrate reversible light-induced electroporation. This process can be extended to allow for on-chip gene

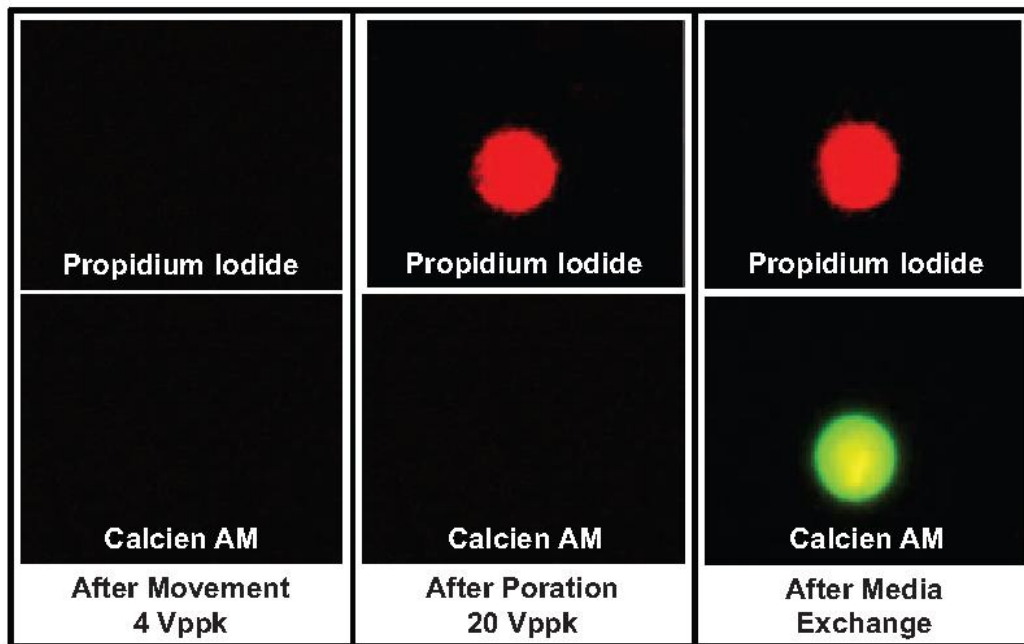


Figure 8: Fluorescent response of cell in Figure 7 for both PI and CaAM. Initially, the cell is suspended in a solution only containing PI ($6\mu\text{M}$). In the first panel, no dye uptake is observed following positioning of the cell with OET at 4 Vppk. In the second panel, the cell is subjected to the electroporation bias resulting in PI dye uptake. In the third panel, the media is exchanged using microfluidic channels with a solution containing CaAM ($2\mu\text{M}$). The cell now exhibits CaAM and PI response verifying successful reversible electroporation.

transfection and cell culture, eventually leading to a high throughput electroporation assay with single cell selectivity.

ACKNOWLEDGEMENTS

The authors would like to thank Ann Fischer of the UC Berkeley Cell Culture Facility for providing the cells. This work was funded by the Center for Cell Control, a National Institute of Health Nanomedicine Development Center, Grant # PN2 EY018228.

REFERENCES

- [1] H. Q. He, D. C. Chang, and Y. K. Lee, "Using a micro electroporation chip to determine the optimal physical parameters in the uptake of biomolecules in HeLa cells," *Bioelectrochemistry*, vol. 70, pp. 363-368, May 2007.
- [2] H. Y. Wang and C. Lu, "Microfluidic electroporation for delivery of small molecules and genes into cells using a common DC power supply," *Biotechnology and Bioengineering*, vol. 100, pp. 579-586, Jun 2008.
- [3] M. Khine, C. Ionescu-Zanetti, A. Blatz, L. P. Wang, and L. P. Lee, "Single-cell electroporation arrays with real-time monitoring and feedback control," *Lab on a Chip*, vol. 7, pp. 457-462, 2007.
- [4] J. K. Valley, H. Y. Hsu, A. T. Ohta, S. Neale, A. Jamshidi, and M. C. Wu, "In-situ Single Cell Electroporation Using Optoelectronic Tweezers," in *IEEE/LEOS Optical MEMS*, Freiburg, Germany, 2008.
- [5] P. Y. Chiou, A. T. Ohta, and M. C. Wu, "Massively parallel manipulation of single cells and microparticles using optical images," *Nature*, vol. 436, pp. 370-372, Jul 21 2005.
- [6] S. W. Hui, "Effects of Pulse Length and Strength on Electroporation Efficiency," in *Animal Cell Electroporation and Electrofusion Protocols*, vol. 48, J. A. Nickoloff, Ed.: Humana Press, 1995, pp. 29-40.
- [7] J. S. Soughayer, T. Krasieva, S. C. Jacobson, J. M. Ramsey, B. J. Tromberg, and N. L. Allbritton, "Characterization of Cellular Optoporation with Distance," *Anal. Chem.*, vol. 72, pp. 1342-1347, 2000.